

(5) pd 26-09-1999

# NOVEL FIBRE DESIGN FOR NARROW-BAND SYMMETRIC RESPONSE SIDETAP FILTERS WITH SUPPRESSED LEAKY MODE RESONANCE

XP-001004571

M J Holmes(1), R Kashyap(2), R Wyatt(2) and R P Smith(2)

- (1) Electronics Dept., King's College London, Strand, London WC2R 2LS. E-mail: [melanie.j.holmes@kcl.ac.uk](mailto:melanie.j.holmes@kcl.ac.uk)  
(2) BT Labs, Martlesham Heath, Ipswich, Suffolk IP5 3RE. E-mail: [raman.kashyap@bt-sys.bt.co.uk](mailto:raman.kashyap@bt-sys.bt.co.uk)

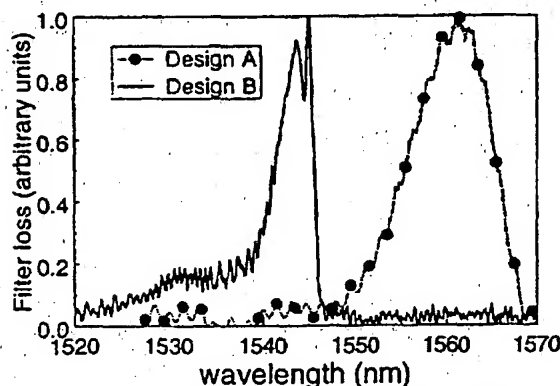
*Abstract: We present a new fibre structure for use in sidetap filters for telecommunications applications, with a symmetric wavelength response, a FWHM bandwidth of only 5 nm and extinction of the leaky mode resonance.*

## Introduction

P 216-217 (2)  
A sidetap grating is a Bragg grating written inside an optical fibre with fringe planes that are blazed with respect to the optical axis [1]. A sidetap grating acts as a wavelength-dependent reflector, as does any Bragg grating. However, the blaze angle of the sidetap grating causes the reflected light to leave the fibre core at an angle that depends on a resonance condition between the wavelength, blaze angle and period of the fringes. Hence a sidetap grating acts as a wavelength-dependent loss filter with applications in gain-flattening of optical amplifiers, pump blocking filters, channel blocking filters, wavelength monitoring etc.

Recently [2] we presented a new design for an optical fibre sidetap filter using fibre and grating designs yielding a very narrow filter response (a measured FWHM bandwidth of 4 nm). The narrow bandwidth was obtained by tailoring the 'photosensitivity profile' to provide a fibre with a non-photosensitive fibre core and a photosensitive cladding. Low backreflection was maintained by the appropriate choice of blaze angle, while low splice loss and insensitivity to bends was obtained by using non-photosensitive index dopants to provide a refractive index profile, and core-cladding index difference,  $\Delta N$ , compatible with standard fibre.

**Figure 1 : Comparison of experimental results for two different filter designs, A and B. Both designs have a step refractive index profile, with a V number close to 2. Design A is for  $\Delta N = 0.003$  and a photosensitive core, while design B is for  $\Delta N = 0.0045$  and a photosensitive cladding.**



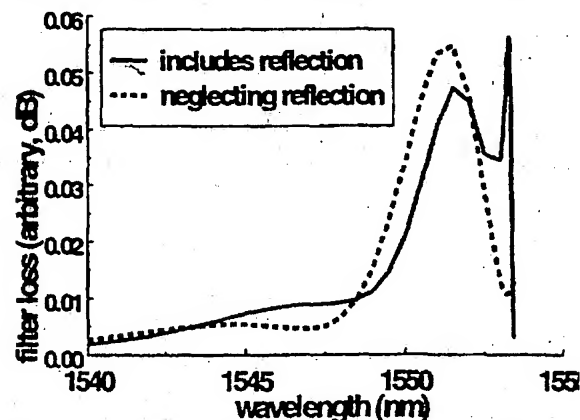
Measured loss spectra for two different fibre designs are compared in figure 1. For both designs the refractive index profile is step-index, but the  $\Delta N$  values are not the same. Design A uses a photosensitive core with a non-photosensitive cladding, and a  $\Delta N$  of 0.003. This non-standard  $\Delta N$  was used in order to reduce the filter bandwidth. Design B uses a non-photosensitive core and a photosensitive cladding, with a  $\Delta N$  of 0.0045: to obtain such a narrow wavelength response with normally photosensitive fibre the  $\Delta N$  would have to be below 0.001. However, ideally we would wish the wavelength response to be symmetric about the main peak: for both designs the

wavelength response is asymmetric about the (main) peak, although the asymmetry is much stronger for design B. A feature of design B is the presence of a strong resonance at wavelengths above the main peak. The aim of our recent research in this area has been to design filters with a symmetric response and without this resonance at long wavelengths.

## Effect of the core-cladding boundary

In our earlier work we used a simple theoretical model based on antenna theory [3] in the Fraunhofer limit, with modifications to take into account the longitudinal variation of the field incident on the grating, due to the light that has already been scattered [4]. In this model the effect of the core-cladding boundary on the properties of the filter was ignored, in order to obtain a first approximation to the filter performance. From a coupled-mode theory perspective, this approximation is equivalent to taking into account coupling into radiation modes, but neglecting coupling into leaky modes [3]. Our earlier model did not predict the strong secondary resonance shown in figure 1, and hence we attributed it to a leaky mode resonance. Subsequently we have extended our model to take into account the effect of the core-cladding boundary, adapting the antenna theory of Ref. 3 to the case of a grating written inside an arbitrary region of the fibre cross-section.

**Figure 2 : Comparison of theoretical results for design B.**



The predictions of the two models are compared in figure 2, for design B. Comparison with figure 1 shows that the predictions of the new model are in good agreement with the measurements for both the short wavelength shoulder and the sharp resonance at long wavelengths. The new model was then used to investigate the effects of further changes to the fibre and grating designs, in order firstly to suppress the leaky mode resonance and secondly to make the filter response symmetric about the peak.

## Suppressing the leaky mode resonance

Numerical simulations have been used to investigate the effect of the fibre V number on the wavelength response,

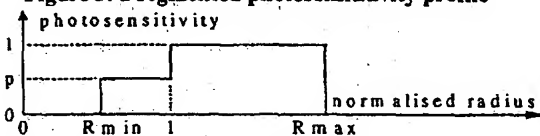


and it was found that for all photosensitivity profiles investigated, the leaky mode resonance could be suppressed by reducing the fibre V number to 1.7.

#### Design modifications for a symmetric response

The symmetric response was achieved by defining a segmented photosensitivity profile, as shown in figure 3. This new photosensitivity profile has a uniformly photosensitive cladding, out to a normalised radius  $R_{max}$ , and a partially photosensitive core, down to a normalised radius  $R_{min}$ , and with a relative photosensitivity of  $p$ , compared to the cladding. As in design B, the index dopants are assumed to provide a refractive index profile compatible with standard fibre.

Figure 3: a segmented photosensitivity profile



Numerical simulations were carried out to find the optimum values of the parameters  $R_{min}$ ,  $R_{max}$  and  $p$ . For every design evaluated, the blaze angle was adjusted to correspond with the first zero in the backreflection [5].

Figure 4: Filter loss spectra as a function of the inner radius,  $R_{min}$ , of the segmented photosensitivity profile, for the same photosensitivity in the core and cladding, and a step refractive index profile with  $V = 1.7$  and  $\Delta N = 0.0045$ .

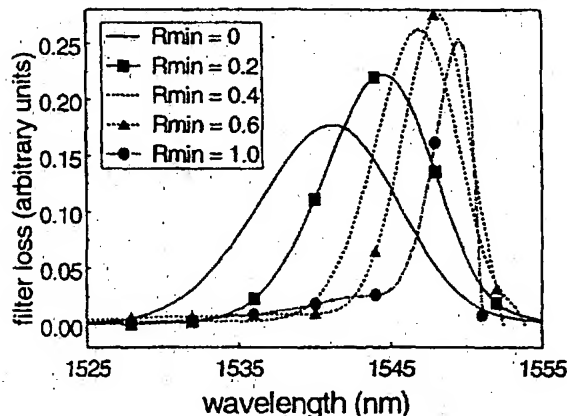


Figure 5: Filter loss spectra as a function of the relative photosensitivity,  $p$ , of the inner annulus of the segmented photosensitivity profile, for  $R_{min}=0.4$ ,  $R_{max}=3.5$  and a step refractive index profile with  $V=1.7$  and  $\Delta N=0.0045$ .

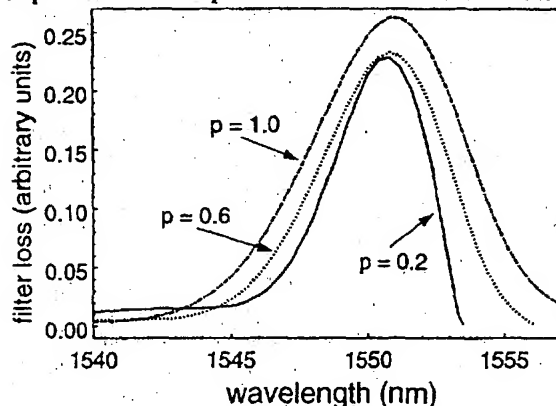


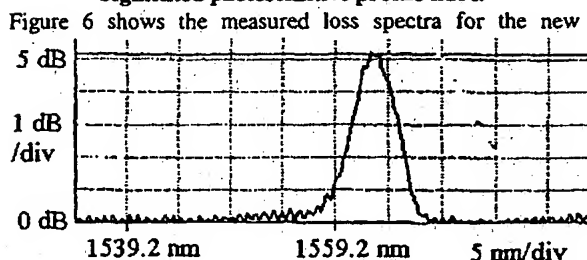
Figure 4 shows the effect of varying  $R_{min}$ , for  $R_{max}$  of 3.5,  $V=1.7$  in order to keep the leaky mode resonance suppressed, and the same photosensitivity in the fibre core and cladding ( $p=1$ ). The results show that decreasing  $R_{min}$  from 1 (as also in design B, figures 1 and 2) has the effect of removing the short wavelength shoulder and hence making the spectra more symmetric, but also increasing the filter

bandwidth. The optimum value of  $R_{min}$  is around 0.4: below this value the spectra are much wider, and above this value the shoulders appear. However, compared to design B (figures 1 and 2) the FWHM bandwidth has increased to 6.5 nm. The next stage in the design was to investigate the effect of varying the relative photosensitivity inside the fibre core (the parameter  $p$  in figure 3). The results are plotted in figure 5, and show that the effect of reducing the relative photosensitivity inside the fibre core is to reduce the filter bandwidth but at low  $p$ , the short wavelength shoulder and asymmetry in the main peak reappear. The optimum value of  $p$  is around 0.6 for which the FWHM bandwidth is 5.5 nm: below this value of  $p$  the filter loses its symmetry and above this value of  $p$  the main peak is broader.

#### Results

With reference to figure 3, a fibre preform was made using a non-photosensitive core dopant for normalised radius less than 0.4, a combination of a non-photosensitive core dopant and germania for normalised radius in the range [0.4,1], and a photosensitive cladding doped with germania out to a normalised radius of 3.5, to which boron was added in order to reduce the cladding index to match the deposition tube. The relative molecular concentrations of germania for the regions [0.4, 1] and [1, 3.5] were in the ratio 0.6:1 in order to obtain the required relative photosensitivity. The preform was drawn into a fibre and hydrogenated. Fibre gratings were written using a 244 nm UV laser and a phase mask [6].

Figure 6: The transmission loss spectra of the new segmented photosensitive profile fibre.



structure: the measured bandwidth is only 5 nm. Compared to design B (figures 1 and 2), the short wavelength shoulder and the leaky mode resonance have been very well suppressed. The smooth, narrow symmetric transmission loss spectrum is ideally suited for optical amplifier gain flattening applications.

#### Conclusions

We have demonstrated both theoretically and experimentally, a new design of photosensitive fibre that is suited for narrow band symmetric filter applications such as gain flattening. This design shows that the leaky mode resonances may be suppressed. These fibres have reasonably low bend loss sensitivity, and are well matched with standard telecommunications fibres.

#### References

- [1] Kashyap R, Wyatt R and McKee P F, "Wavelength flattened saturated erbium amplifier using multiple side-tap Bragg gratings", *Electron. Lett.* 29(11), 1025, 1993.
- [2] Holmes M J, Kashyap R, Smith R P and Wyatt R, "Ultra narrowband optical fibre sidetap filters", *Proc ECOC 98*, Madrid, September 1998, pp 137-138.
- [3] Snyder A W and Love J D, "Optical Waveguide Theory", Chapman and Hall, London, 1983.
- [4] Holmes M J, Kashyap R and Wyatt R, "Physical properties of optical fibre sidetap grating filters: free space model, *JSTQE*, accepted for publication September 1999.
- [5] Erdogan T and Sipe J E, "Tilted fiber phase gratings", *J. Opt. Soc. Am. A*, 13, 296-313, 1996.
- [6] Kashyap R, Armitage J R, Campbell R J, Maxwell G D, Williams D L, Ainslie B J and Millar C A, "Light sensitive fibres and planar waveguides", *Br. Telecom. Technol. J.* 11 (2), April 1993.



# Narrow-Band Rejection Filters with Negligible Backreflection Using Tilted Photoinduced Gratings in Single-Mode Fibers

Charles W. Haggans, Harmeet Singh, Wayne F. Varner, Yaowen Li, and Mark Zippin

XP-000754661

**Abstract**—Suppression of the forward propagating  $LP_{01}$  core mode of  $>17$  dB with  $<-30$ -dB backreflection over a narrow wavelength band is demonstrated utilizing a tilted photoinduced Bragg grating in a deep depressed inner cladding single-mode fiber (SMF). Theoretical and experimental results detailing the tilted grating filter performance in matched cladding, depressed inner cladding, and photosensitive cladding SMF's are presented.

**Index Terms**—Bragg scattering, gratings, optical fiber filters, optical fiber cladding, wavelength-division multiplexing.

## I. INTRODUCTION

A PASSIVE component in a single-mode fiber (SMF) that suppresses the forward propagating  $LP_{01}$  core mode over a narrow wavelength band with negligible backreflection is a critical filtering element for lightwave systems in which no backreflected signal can be tolerated. Most previous efforts toward obtaining narrow-band rejection filters utilizing fiber gratings have obtained the loss via coupling to the counterpropagating  $LP_{01}$  core mode, giving rise to a large backreflected signal. Other filtering approaches can be broken into two categories: coupling to the  $LP_{11}$  mode in a two mode fiber [1]–[4] and coupling to cladding or radiation modes in a SMF [5]–[11].

Recently, Strasser *et al.* [3] demonstrated suppression of the forward propagating  $LP_{01}$  core mode over a narrow wavelength band in a two mode fiber utilizing a fiber grating. In that work, the backreflected signal at the peak rejection wavelength was  $\sim -15$  dB, which is larger than the desired isolation for components in many lightwave communication systems.

In this letter, we demonstrate gratings in depressed inner cladding (DIC) and photosensitive matched inner cladding (PMIC) SMF's that allow for narrow-band rejection filtering in transmission with  $<-30$  dB backreflection at the peak rejection wavelength. The primary advantage of these fiber designs over matched clad (MC) fiber designs for this filter type (tilted gratings in SMF's) is that low insertion losses are obtained in a narrow wavelength band to the short wavelength side of

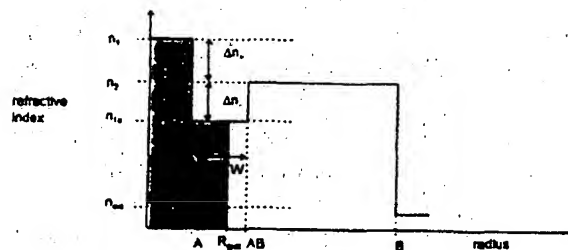


Fig. 1. Radial distribution of refractive index for depressed and photosensitive clad fibers. The shaded region corresponds to the photosensitive region of the fiber.

the rejection band. We utilize this property of these filters in demonstrating a low-reflection channel-block bandpass filter.

## II. FIBER AND GRATING DESIGN

Strong grating-induced coupling between the core and counterpropagating cladding modes has been previously observed in a shallow depressed inner clad fiber (AT&T Accutether) by Hewlett *et al.* [12]. This coupling is enabled through a physical tilt of the grating fringes or other azimuthally asymmetric grating strength across the core, which has a component of the azimuthal symmetry proportional to  $\cos \varphi$ . This coupling can be quantified in the case of a tilted grating through the use of a relative coupling coefficient (RCC) [13] in (1), at the bottom of the next page, where  $\theta$  is the in-fiber grating tilt angle,  $\Lambda$  is the grating period,  $R_{\text{grat}}$  is the radius of maximum extent of the grating, and  $\psi_{01}(r, \varphi)$  and  $\psi_{Lm}(r, \varphi)$  are the normalized LP transverse field distributions [14].

For the DIC fiber geometry (as detailed in Fig. 1 but with  $R_{\text{grat}} = A$ ), a wide, deep depressed inner cladding gives strong coupling to the  $LP_{11}$  hybrid mode of Hewlett *et al.* [12] (strong  $LP_{01} = LP_{1m}$  coupling). By plotting the maximum value of  $RCC_{1m}$  ( $1 \leq m \leq 30$ ) versus  $\Delta n_2$  and  $W$  for a range of tilt angles (e.g.,  $\theta = 1^\circ, 3^\circ, 5^\circ$ ), limits on  $W$  and  $\Delta n_2$  for obtaining strong coupling can be determined. For example, at an operating wavelength of 1550 nm with fiber parameters consistent with standard matched clad (MC) telecommunication fiber, strong coupling is obtained for  $W > 0.6 A$  and  $\Delta n_2 > 0.003$ . The tilt angle for optimum suppression of  $LP_{01} = LP_{01}$  coupling is then determined by minimizing  $RCC_{01}$  with respect to  $\theta$ . At this angle, power is efficiently coupled from the forward propagating  $LP_{01}$  mode

Manuscript received December 3, 1997; revised January 27, 1998.

C. W. Haggans and W. F. Varner are with 3M Fiber Optics Laboratory, 3M Center, St. Paul, MN 55125 USA.

H. Singh, Y. Li, and M. Zippin are with 3M Bragg Grating Technologies, Bloomfield, CT 06002 USA.

Publisher Item Identifier S 1041-1135(98)03045-6.

to the counterpropagating  $LP_{11}$  hybrid mode. Since the  $LP_{11}$  hybrid mode is lossy, this power is lost from the fiber core over distance, giving narrow-band filtering with negligible backreflection.

In the PMIC fiber geometry (Fig. 1 with  $n_{1a} = n_2$  and  $\gamma = (\text{cladding grating strength})/(\text{core grating strength}) \neq 0$ ), the mechanism for strong  $LP_{01} - LP_{1m}$  coupling is the extension of the grating into the cladding region, giving increased overlap of certain  $LP_{1m}$  modes with the  $LP_{01}$  core mode. By analyzing  $RCC_{1m}$  versus  $R_{\text{grat}}$  and  $\gamma$  for a range of  $\theta$  values, the process proceeds as in the DIC case. From this analysis, strong coupling is obtained for  $R_{\text{grat}} > 1.5 \text{ A}$  and  $\gamma > 0.5$ , and the lossy nature of the  $LP_{1m}$  cladding modes once again gives negligible backreflection for the appropriate tilt angle.

### III. RESULTS

To demonstrate the properties of appropriately designed tilted gratings written in wide depressed inner clad (DIC) and photosensitive matched inner clad (PMIC) fibers, gratings with a center wavelength of  $\sim 1550 \text{ nm}$  were written as a function of tilt angle in three SMF's: 1) MC ( $\Lambda \sim 4.15 \text{ }\mu\text{m}$ , mode field diameter (MFD)  $\sim 10.5 \text{ }\mu\text{m}$ ,  $\Delta n_+ \sim 0.0046$ ); 2) DIC ( $\Lambda = 5.86 \text{ }\mu\text{m}$ ,  $W = 3.85 \text{ }\mu\text{m}$ ,  $\Delta n_+ = 0.0038$ ,  $\Delta n_- = 0.0064$ , MFD  $= 9.5 \text{ }\mu\text{m}$ ); and 3) PMIC ( $\Lambda = 4.7 \text{ }\mu\text{m}$ ,  $\Delta n_+ = 0.0052$ ,  $R_{\text{grat}} = 9.4 \text{ }\mu\text{m}$ ,  $\gamma \sim 1.0$ , MFD  $= 10.1 \text{ }\mu\text{m}$ ). The gratings written were 15 mm in length, unapodized, and the spectra were measured after recoating ( $n_{\text{ext}} \sim n_2$ ). The gratings were written after hydrogen loading using a sidewriting phase mask exposure technique with an excimer laser at 248 nm with a total dose sufficient to give approximately  $-20 \text{ dB}$  losses in transmission. A variable in-fiber fringe tilt angle ( $\theta$ ) was achieved by orienting the phase mask rulings at an angle of  $\theta' = 90^\circ + \theta/n_2$  from the fiber axis. Note that the  $1/n_2$  factor is included as a first-order correction for the lensing effect of the fiber.

Transmission spectra for gratings written in these three fibers with  $\theta = 0^\circ$  and  $3.6^\circ$  are plotted in Fig. 2. The grating spectra for all three fiber types with  $\theta = 0^\circ$  exhibit similar  $LP_{01} - LP_{01}$  coupling (fundamental) rejection notches, with corresponding strong backreflected signals at the peak rejection wavelengths. The fundamental rejection notches for the  $\theta = 0^\circ$  and  $3.6^\circ$  MC fiber spectra are also similar in shape, with the notch for the  $3.6^\circ$  spectrum shifted to longer wavelengths due to the tilt-induced effective period increase. However, strong overlapping loss peaks due to  $LP_{01} - LP_{0m}$  and  $LP_{01} - LP_{1m}$  cladding mode coupling are present in the  $3.6^\circ$  MC spectrum, with the peak cladding mode loss occurring near  $1552 \text{ nm}$ . While this loss peak could conceivably be used in a nonreflecting filter application, it would not be useful

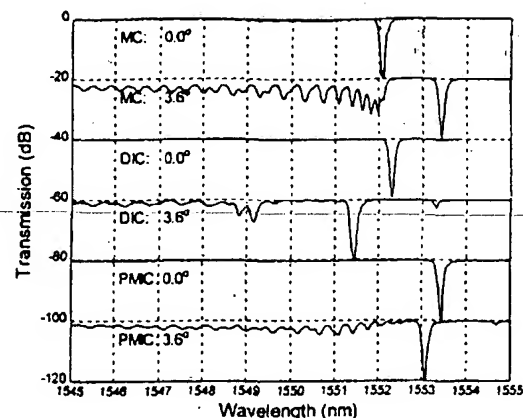


Fig. 2. Transmission spectra versus tilt angle for MC, DIC, and PMIC fibers. Individual spectra are displaced from nearest neighbors by  $\pm 20 \text{ dB}$  for ease in visualization.

in multigrating cascades for channel-block filter applications, because there is no low-loss region to the shorter wavelength side of the loss peak.

For the DIC and PMIC fibers, the  $\theta = 3.6^\circ$  spectra have characteristics that are desirable for nonreflecting narrow-band rejection filters. In the  $3.6^\circ$  spectra, the undesirable loss notches due to  $LP_{01} - LP_{01}$  coupling are shifted to higher wavelengths than in the  $0^\circ$  spectra ( $1553.2$  and  $1554.7 \text{ nm}$ , respectively), and are substantially weakened. Additionally, the desirable strong loss notches due to  $LP_{01} - LP_{1m}$  coupling are visible centered at  $1551.5 \text{ nm}$  for the DIC fiber and  $1553.1 \text{ nm}$  for the PMIC fiber. Finally, a relatively low-loss region exists to the short wavelength side of these notches for the DIC and PMIC  $3.6^\circ$  spectra, in contrast to the  $3.6^\circ$  MC spectrum. The width of this low-loss region is approximately  $2 \text{ nm}$  for the DIC grating and approximately  $1 \text{ nm}$  for the PMIC grating. These low loss bands occur due to the  $LP_{01} - LP_{0m}$  coupling suppression qualities of DIC and PMIC fibers [15]–[16].

To illustrate the reflection and transmission properties of a DIC filter design with a suppressed fundamental notch, Fig. 3 is a plot of the transmission and reflection spectra for a grating with  $\theta = 4^\circ$  written in the DIC fiber. On this plot, the transmission minimum due to  $LP_{01} - LP_{01}$  coupling at  $\lambda \sim 1554 \text{ nm}$  is not distinguishable. The  $\sim 2\text{-nm}$  passband between the higher order loss notches ( $\lambda < 1550.25 \text{ nm}$ ) and the peak  $LP_{01} - LP_{1m}$  loss notch ( $\lambda = 1552.25 \text{ nm}$ ) allows for the application of this device in some bandpass filter applications. The reflection spectrum in Fig. 3 demonstrates that reflection due to  $LP_{01} - LP_{01}$  coupling ( $\lambda \sim 1554 \text{ nm}$ ) is  $< -20 \text{ dB}$ . However, reflection in the rejection band is  $< -30 \text{ dB}$ .

From the results of Figs. 2 and 3, it can be anticipated that the PMIC fiber design also reaches an angle where the

$$RCC_{Lm} = RCC_{01,Lm} = \frac{\left| \int_0^{2\pi} \int_0^{R_{\text{grat}}} \psi_{01}^*(r) \psi_{Lm}(r, \varphi) \exp \left[ -\frac{i2\pi}{\Lambda} \sin \theta r \cos \varphi \right] r dr d\varphi \right|}{\left| \int_0^{2\pi} \int_0^{\Lambda} |\psi_{01}(r)|^2 r dr d\varphi \right|} \quad (1)$$

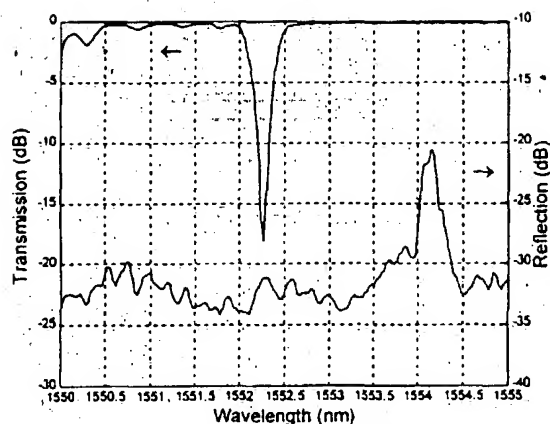


Fig. 3. Transmission and reflection spectra for DIC fiber for in fiber fringe tilt of  $\theta = 4.0^\circ$ .

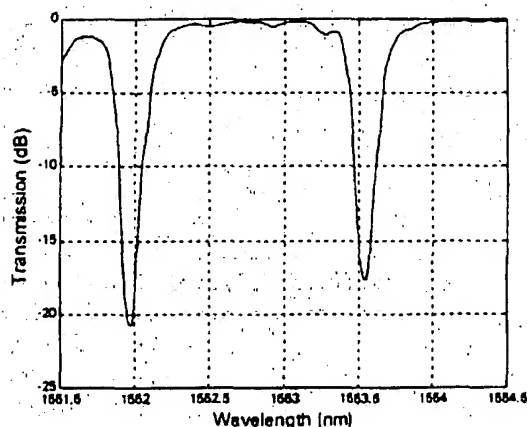


Fig. 4. Transmission spectrum for channel-block bandpass filter formed by cascading two gratings of the type detailed in Fig. 5.

fundamental is strongly suppressed. This suppression occurs for  $\theta \sim 3.7^\circ$ . At this operating point, strong rejection performance can also be achieved, but with a smaller passband to shorter wavelengths than for the DIC fiber, as discussed above. Finally, the width of the rejection notch in Figs. 2 and 3 may be increased by chirping the grating, and the performance of the DIC design can be enhanced by adding photosensitivity to the cladding regions.

Narrow-band filters of this type have numerous applications in lightwave systems such as bandpass filtering, test signal dropping, and gain flattening. As an example, a channel-block bandpass filter for a 100-GHz channel spacing WDM system can be generated by cascading two filters with spectra similar to that of Fig. 3, but different peak rejection wavelengths. Fig. 4 shows the transmission spectrum for the two grating

cascade, which exhibits the desired strong rejection for channels at  $\sim 1552$  and  $\sim 1553.6$  nm and small insertion loss for the channel at  $\sim 1552.8$  nm.

#### IV. CONCLUSION

A novel narrow-band suppression filter with  $< -30$  dB backreflection and  $> 17$ -dB suppression in transmission in an SMF has been demonstrated. Additionally, a channel-block bandpass filter generated using two cascaded gratings has been demonstrated.

#### REFERENCES

- [1] H. Park and B. Kim, "Intermodal coupler using permanently photoinduced grating in two-mode optical fiber," *Electron. Lett.*, vol. 25, pp. 797-799, 1989.
- [2] K. O. Hill, B. Malo, K. A. Vineberg, F. Bilodeau, D. C. Johnson, and I. Skinner, "Efficient mode conversion in telecommunication fiber using externally written gratings," *Electron. Lett.*, vol. 26, pp. 1270-1272, 1990.
- [3] T. A. Strasser, J. R. Pedrazzani, and M. J. Andrejco, "Reflective-mode conversion with UV-induced phase gratings in two-mode fiber," in *OFC'97 Tech. Dig.*, 1997, pp. 348-349.
- [4] D. Jochen, P. Klose, A. Ewald, and E. Brinkmeyer, "Non-reflecting narrow-band fiber optical Fabry-Perot transmission filter," in *Bragg Gratings, Photosensitivity, and Poling in Glass Fibers and Waveguides: Applications and Fundamentals*, vol. 17. Washington, DC: Opt. Soc. Amer., 1997, pp. 42-44.
- [5] J. A. Aberson, Jr. and I. A. White, "Device for tapping radiation from, or injecting radiation into, single mode optical fiber, and communication system comprising same," U.S. Patent 4 749 248, 1988.
- [6] R. E. Epworth, S. Wright, R. J. Brambley, and D. F. Smith, "Devices and methods for selectively tapping optical energy from an optical fiber," U.S. Patent 4 781 428, 1988.
- [7] G. Meltz and W. W. Morey, "Design and performance of bidirectional fiber Bragg grating taps," in *Proc. OFC'91*, 1990, p. 44, paper TuM2.
- [8] R. Kashyap, R. Wyatt, and R. J. Campbell, "Wideband gain flattened erbium fiber amplifier using a photosensitive fiber blazed grating," *Electron. Lett.*, vol. 29, pp. 154-156, 1993.
- [9] A. M. Vengsarkar, "Optical systems and devices using long period spectral shaping devices," U.S. Patent 5 430 817, 1995.
- [10] V. Mizrahi, "Optical waveguiding component comprising a band-pass filter," U.S. Patent 5 570 440, 1996.
- [11] P.-Y. Fonjallaz, H. G. Limberger, and R. P. Salathe, "Bragg gratings with efficient and wavelength-selective fiber out-coupling," *J. Lightwave Technol.*, vol. 15, pp. 371-376, 1997.
- [12] S. J. Hewlett, J. D. Love, G. Meltz, T. J. Bailey, and W. W. Morey, "Coupling characteristics of photo-induced Bragg gratings in depressed- and matched-cladding fiber," *Opt. Quantum Electron.*, vol. 28, pp. 1641-1654, 1996.
- [13] J. L. Archambault, "Photorefractive gratings in optical fibers," Ph.D. dissertation, Univ. of Southampton, U.K., 1994, ch. 2.
- [14] A. W. Snyder and J. D. Love, *Optical Waveguide Theory*. London, U.K.: Chapman and Hall, 1983, ch. 13.
- [15] L. Dong, L. Reekie, J. L. Cruz, J. E. Caplen, J. P. de Sandro, and D. N. Payne, "Optical fibers with depressed claddings for suppression of coupling into cladding modes in fiber Bragg gratings," *IEEE Photon. Technol. Lett.*, vol. 9, pp. 64-66, 1997.
- [16] E. Delevaque, S. Boj, J. F. Bayon, H. Poignat, J. Le Mellot, and M. Monerie, "Optical fiber design for strong gratings photoimprinting with radiation mode suppression," presented at the Optical Fiber Communication Conf., 1995, paper PD5.

-----

-----

-----

-----